

Geophysical Research Letters

RESEARCH LETTER

10.1029/2019GL085980

Key Points:

- The steady-state radius of maximum wind r_m has a linear relationship to the absolute angular momentum M_m that $r_m = aM_m + b$
- The nonnegligible intercept b is responsible for the various steady-state maximum intensities
- Horizontal turbulent mixing acts a role on the steady-state maximum intensities through adjusting the linear relationship between r_m and M_m

Supporting Information:

- Supporting Information S1

Correspondence to:

D. Tao,
ddantao@colostate.edu

Citation:

Tao, D., Bell, M., Rotunno, R., & van Leeuwen, P. J. (2020). Why do the maximum intensities in modeled tropical cyclones vary under the same environmental conditions?. *Geophysical Research Letters*, 47, e2019GL085980. <https://doi.org/10.1029/2019GL085980>

Received 6 NOV 2019

Accepted 7 JAN 2020

Accepted article online 22 JAN 2020

Why Do the Maximum Intensities in Modeled Tropical Cyclones Vary Under the Same Environmental Conditions?

Dandan Tao¹, Michael Bell¹, Richard Rotunno², and Peter Jan van Leeuwen¹

¹Department of Atmospheric Science, Colorado State University, Fort Collins, CO, USA, ²National Center for Atmospheric Research, Boulder, CO, USA

Abstract In this study we explored why the different initial tropical cyclone structures can result in different steady-state maximum intensities in model simulations with the same environmental conditions. We discovered a linear relationship between the radius of maximum wind (r_m) and the absolute angular momentum that passes through r_m (M_m) in the model simulated steady-state tropical cyclones that $r_m = aM_m + b$. This nonnegligible intercept b is found to be the key to making a steady-state storm with a larger M_m more intense. The sensitivity experiments show that this nonzero b results mainly from horizontal turbulent mixing and decreases with decreased horizontal mixing. Using this linear relationship from the simulations, it is also found that the degree of supergradient wind is a function of M_m as well as the turbulent mixing length such that both a larger M_m and/or a reduced turbulent mixing length result in larger supergradient winds.

Plain Language Summary According to the maximum potential intensity theory, the maximum intensities for tropical cyclones should be the same given the same environmental conditions, which means the radius of maximum wind (r_m) at the boundary layer top should be linearly proportional to the absolute angular momentum such that $r_m \sim aM_m$. In model simulations, however, different initial vortex structures usually result in different quasi-steady-state maximum intensities. In this paper, an axisymmetric numerical model is used to evaluate the TC's maximum intensities at the quasi-steady state and explore the cause of this discrepancy between the model simulations and the maximum potential intensity theory. The model results exhibit that the various values of r_m do have a linear relation with M_m , which is predicted by the maximum potential intensity theory. However, there is a non-negligible intercept term, b , in this linear relation ($r_m = aM_m + b$), which is found to be the key to making a steady-state storm with a larger M_m more intense.

1. Introduction

The size and intensity of tropical cyclones (TCs) as well as their relationship have been explored by many modeling and observational studies. Merrill (1984) found that the radius of outermost closed isobar is weakly correlated to a TC's intensity. Meanwhile, the statistical analysis shows that the intensification rate has a weak negative correlation with the radius of maximum wind and the radius of gale-force wind (Carrasco et al., 2014; Xu & Wang, 2015). It is also found through idealized model simulations that the size of a mature TC is highly dependent on the size of its initial vortex (Chan & Chan, 2014; Xu & Wang, 2010). However, the relationship between the TC size and intensity is still unclear due to the complexity of external and internal factors that contribute to their evolution. In order to systematically evaluate the relationship between intensity and size, a more quantitative analysis based on theoretical TC dynamics is needed. Since theoretical work has been well established for steady-state TCs, it is beneficial to first investigate the relationship between the size and intensity of steady-state TCs.

Tropical cyclones theoretically have one maximum potential intensity (MPI; see the supporting information for MPI's two interpretations) in a given environment, which is mainly determined by the environmental parameters (Emanuel, 1986, 1988, 1995; Emanuel & Rotunno, 2011, hereinafter ER11; Shutts, 1981). This environmental control would indicate that the tropical cyclone initial conditions and its internal processes would have little influence on the maximum achievable intensity if the tropical cyclone could develop in the same environment without interruption. This environmental limit on maximum achievable TC

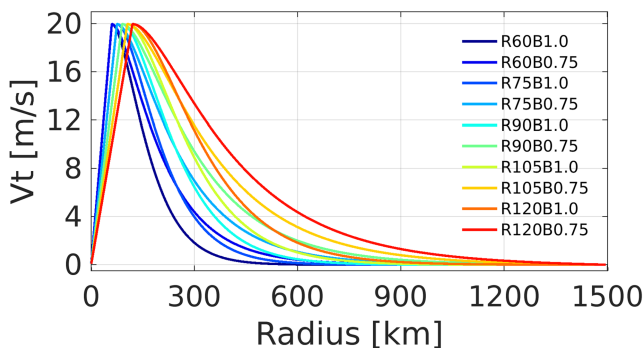


Figure 1. Initial surface tangential wind profiles: a larger B indicates a $V(r)$ that decays faster outside of r_m . The profiles are from equation (1) of Xu and Wang (2018).

the radius of maximum wind, V_m is the maximum tangential wind, M_m is the angular momentum surface that passes through r_m . Since the value of V_m is the same for steady-state storms in the same environment, according to the MPI theories, all of the variation in M_m should be that of r_m and there should exist a linear relationship between M_m and r_m that depends only on environmental conditions. In seeming contradiction of the foregoing theoretical results, the final quasi-steady-state maximum intensities of different initial vortices in the same environment in model simulations are usually significantly different from each other (Rotunno and Emanuel, 1986; Xu & Wang, 2010, 2018). We attempt here to at least partially address this phenomenon in simulated TCs and find the relation among V_m , r_m , and M_m . Section 2 describes the model simulation setup. Section 3 presents the results from the simulations. Summary is provided in section 4. At the end of the paper, we will also discuss the application of this study to better understanding TC intensity and size, and explain the new insights in the forecasting of future TCs.

2. Model Setups

We use the axisymmetric version of the nonhydrostatic Cloud Model, version 1 (CM1), as described in Bryan and Rotunno (2009). The domain is 1,500 km in radius with a grid spacing of 1 km for $r < 300$ km and linearly stretched to 15 km for $r \geq 300$ km. There are 140 vertical levels, with the lowest model level at 25 m above the surface and the highest model level at 25 km. The vertical grid spacing varies from 50 to 200 m for $z < 5$ km and is fixed to 200 m for $z \geq 5$ km. A constant Coriolis parameter ($f = 5 \times 10^{-5} \text{ s}^{-1}$) and a constant sea surface temperature (28 °C) are used. The vertical turbulent mixing length is set to 100 m, while the horizontal turbulent mixing length is set to 1,000 m. There are three sets of experiments with a fixed $C_k = 10^{-3}$ but varying C_d to obtain $\frac{C_k}{C_d} = 0.5, 1.0, 1.5$, respectively (CkCd0.5, CkCd1.0, CkCd1.5). Two extra sensitivity sets with smaller horizontal turbulent mixing lengths (100 and 500 m, respectively; CkCd1.0_lh100, CkCd1.0_lh500) are performed to explore the role of horizontal turbulent mixing in modulating the relation among steady-state M_m , r_m , and V_m .

The radial profiles of the initial surface tangential winds using equation (1) of Xu and Wang (2018) are shown in Figure 1. The initial maximum surface wind is 20 m s⁻¹ for all simulations. There are 5 different initial r_m values ($r_m = 60, 75, 90, 105$, and 120 km, respectively) and two different “skirt” parameters ($B = 1.0$ and 0.75, respectively; a smaller B produces a broader radial profile). The tangential wind vanishes at $r = 1,500$ km. The simulation times are 192 hr for CkCd1.0 and 240 hr for CkCd0.5 and CkCd1.5, which are enough for r_m and V_m to reach a quasi-steady state under current environmental and model setups.

3. Results

The simulation results for the maximum tangential wind at the boundary layer top ($z = 1.55$ km) are shown in the first row of Figure 2. As presented in previous studies (ER11; Bryan, 2012; Peng et al., 2018), a larger $\frac{C_k}{C_d}$ ratio tends to generate a larger final maximum intensity. In addition, we find that for the simulations with the same B within the same $\frac{C_k}{C_d}$ set, the larger the initial r_m is, the larger the maximum intensity is. At the same

intensity can be understood from the consideration of several factors. The maximum achievable intensity is the intensity that can balance the mechanical energy available from the enthalpy input from the ocean through the surface sensible and latent heat fluxes and its dissipation in the boundary layer (Emanuel, 1997). The structure of the TC above the boundary layer is such that the angular momentum surfaces emerging from the boundary layer cannot penetrate the tropopause. This puts a strong constraint on the radial location of the angular momentum surface that passes through the radius of maximum wind, and hence the maximum achievable intensity.

The MPI under the foregoing considerations will be the same for the same environment (detailed derivations are shown in the supporting information). Given that the Coriolis term is much smaller than the tangential wind term at the radius of maximum wind in the expression of absolute angular momentum, we have $M_m = r_m V_m + \frac{1}{2} f r_m^2 \cong r_m V_m$, where r_m is

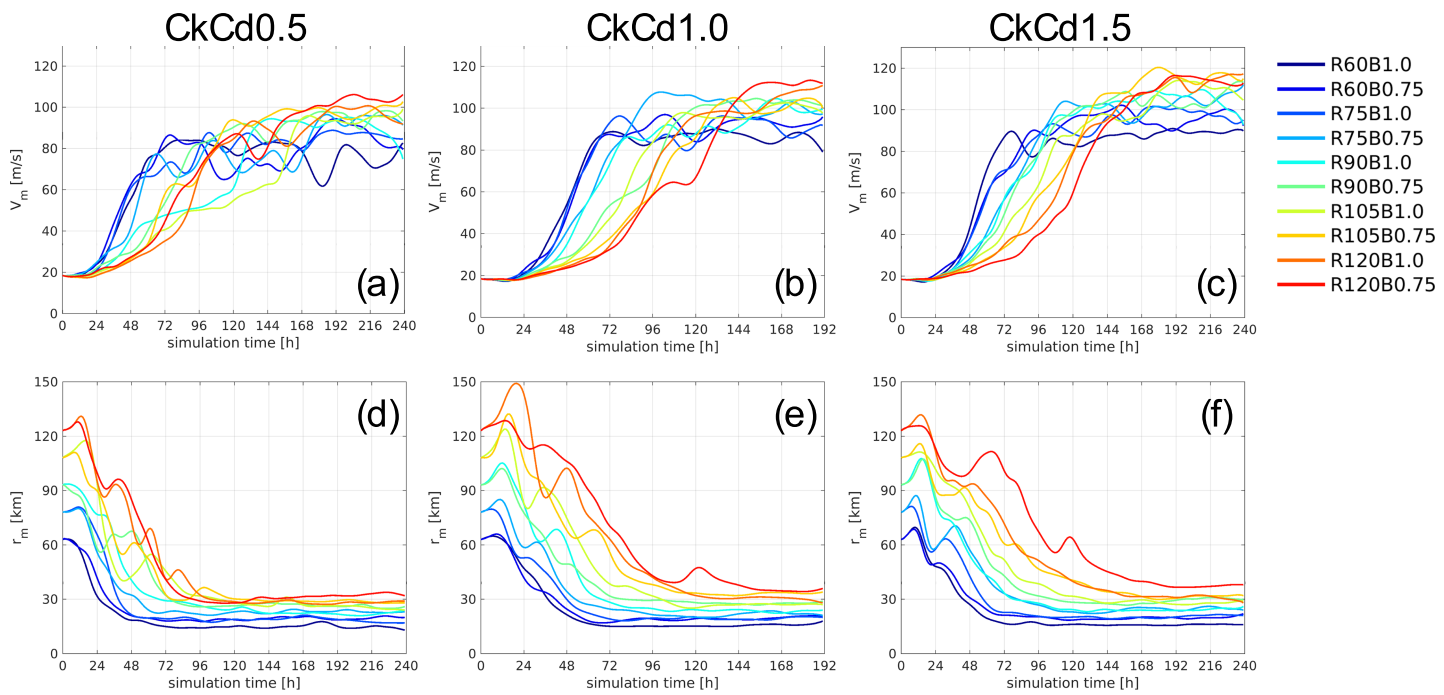


Figure 2. (a–c) Time evolution of the maximum tangential wind at $z = 1.55$ km. (d–f) Time evolution of the radius of maximum wind at $z = 1.55$ km. (left column) CkCd0.5. (middle column) CkCd1.0. (right column) CkCd1.5.

time, the smaller B values (broader initial radial profile) result in larger final maximum intensities for the same initial r_m and the same $\frac{C_k}{C_d}$. The final r_m (second row of Figure 2) is less sensitive to $\frac{C_k}{C_d}$ but quite different among different initial vortex profiles that the values of r_m will keep their ranking order during development, which is consistent with Xu and Wang (2010). While it is not the focus of this study, we also note that the smaller vortices intensify more quickly and reach their final values of r_m sooner than the larger vortices. It is also worth mentioning that given the same initial vortex, the storm takes more time to intensify with a smaller C_d (Bryan, 2013).

According to the MPI theories, we should expect the same maximum intensity for the same $\frac{C_k}{C_d}$ and a linear relationship between r_m and M_m . However, as the first row of Figure 2 shows, the final quasi-steady-state maximum intensities in these simulations under the same environment are significantly different from each other given the different initial storm structures. Generally speaking, in these model simulations, a larger initial vortex will lead to a larger and more intense final vortex given the same environmental conditions.

To further identify the relation among V_m , r_m , and M_m , we plotted r_m as a function of M_m using the values from averaging the last 24 hr of simulation results. Although the same maximum intensity is not observed in Figure 2, linear relationships are found in the model simulations despite the same environmental conditions (first row of Figure 3). We find that

$$r_m = aM_m + b, \quad (1)$$

where a is the slope and b is the r_m intercept, both of which are from the linear regression of the data from the simulated steady-state TCs. The values of a and b vary with $\frac{C_k}{C_d}$ (Table 1). The a value decreases with increasing $\frac{C_k}{C_d}$, which is partially consistent with the expected trend from the MPI theories since $V_m \sim \frac{1}{a}$ in theory. Meanwhile, there is a nonnegligible r_m intercept b in this linear relationship, which is not expected from the MPI theories. In fact, this b is essential to the variation in V_m . It is worth to clarify that this b is not from the Coriolis term in the M_m expression, which is small enough to be neglected at r_m . Using the definition of M_m , we can use the linear relationship (1) to obtain

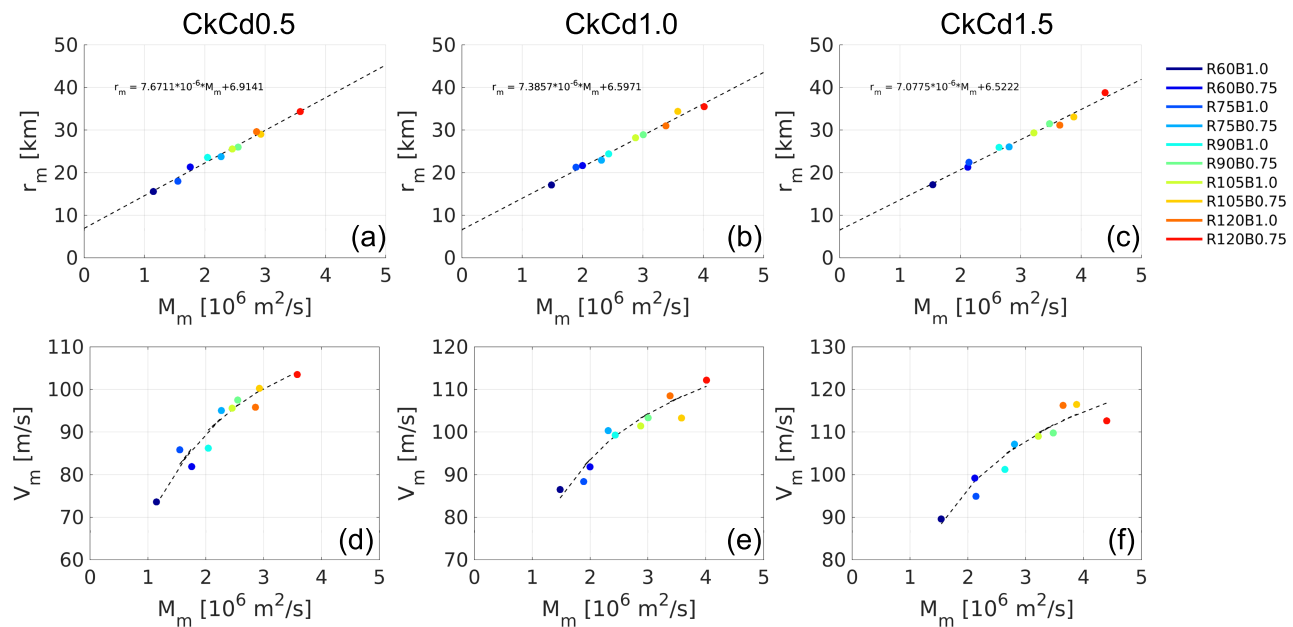


Figure 3. (a–c) Dots are the final 24-hr mean of r_m as a function of the final 24-hr mean of M_m at $z = 1.55$ km. The dash lines are the linear regression of the dots. (d–f) Dots are the final 24-hr mean of maximum tangential wind as a function of the final 24-hr mean of M_m at $z = 1.55$ km. The dash lines are maximum tangential wind calculated from the linear regression of the first row using (2). (left column) CkCd0.5. (middle column) CkCd1.0. (right column) CkCd1.5.

$$V_m \cong M_m / (aM_m + b). \quad (2)$$

The second row of Figure 3 exhibits a good agreement between (2) (dash line) and the model results (dots).

The nonzero intercept parameter b in the linear relationship is indicative of the importance of processes not directly considered in the MPI theory. It is known that the MPI theory assumes an inviscid troposphere above the boundary layer as well as balanced dynamics, which are not satisfied in full-physics model simulations. Here we hypothesize that the discrepancy between analytic theory and the modeling results is mainly due to the neglected horizontal turbulent mixing in the derivation of the analytic solutions. Rotunno and Bryan (2012) found that the horizontal mixing length (l_h) can influence the maximum simulated intensity and radius of maximum wind significantly through redistributing the angular momentum in the inner core region. Zhang and Marks (2015) also found a positive correlation between the radius of maximum wind and the horizontal mixing rate. It is suggested here that a and b could be altered by different horizontal turbulent mixing, which turns out to be the case as shown in Figure 4. The two sensitivity sets (CkCd1.0_lh100 and CkCd1.0_lh500) with smaller horizontal turbulent mixing lengths present that the linear relationship still holds well but with much smaller b , and that b decreases as l_h decreases. The slope parameter a also decreases with smaller l_h , however, the change is less than that in the intercept parameter b . At the same time, the set of CkCd1.0_lh100 generates the highest maximum intensities among CkCd1.0_lh100, CkCd1.0_lh500 and CkCd1.0 not only due to the smaller a and b values (Table 1) but also due to achieving the smallest r_m that M_m can reach with the reduced horizontal turbulent mixing (Figures 3b, 4c, and 4d).

Another application of the linear relationship in equation (1) is to estimate the intensity greater than that given by the MPI theories. The magnitudes of V_m from the present CM1 simulations are much larger than

Table 1
List of a and b values in all sets.

	CkCd0.5	CkCd1.0	CkCd1.5	CkCd1.0_lh100	CkCd1.0_lh500
a [$10^{-6} \text{ km} \cdot \text{s}/\text{m}^2$]	7.67	7.39	7.08	6.44	6.63
b [km]	6.91	6.60	6.52	2.73	5.97

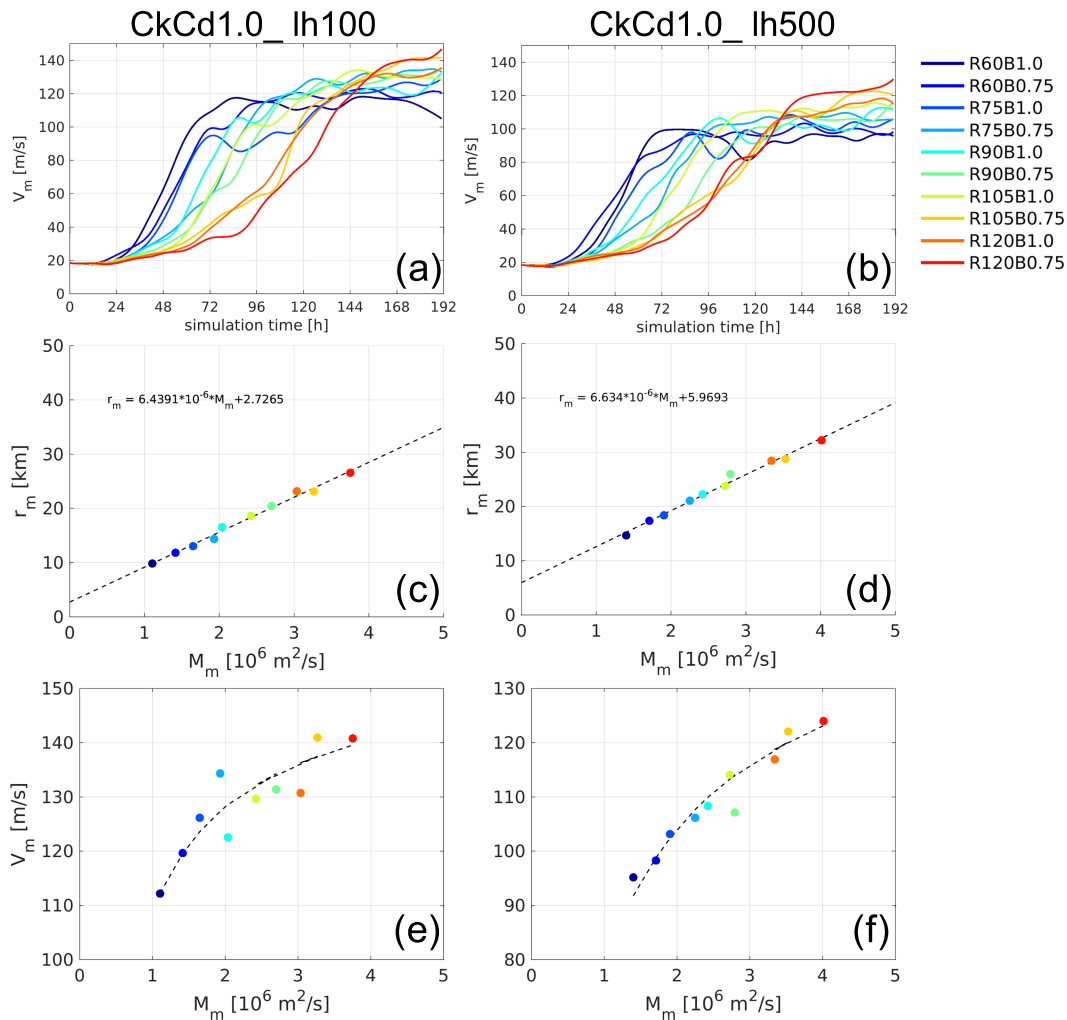


Figure 4. (a and b) Time evolution of the maximum tangential winds at $z = 1.55$ km for CkCd1.0_lh100 and CkCd1.0_lh500. (c–f) The same as Figure 3 but for CkCd1.0_lh100 and CkCd1.0_lh500.

the MPI especially in the smaller turbulent mixing length experiments. Given that the theoretical maximum intensity from balanced assumptions is independent of storm related parameters, we have

$$r_{m0} \approx a_0 M_m, \quad (3)$$

where $a_0 (=1/V_{m0})$ and r_{m0} are the slope and radius of maximum wind from the MPI theories. We use a similar super intensity (SI) index as defined in Rousseau-Rizzi and Emanuel (2019) as

$$SI = \frac{V_m - V_{m0}}{V_{m0}} = \frac{\frac{M_m}{aM_m + b} - \frac{M_m}{a_0 M_m}}{\frac{M_m}{a_0 M_m}} = \frac{a_0}{a + \frac{b}{M_m}} - 1, \quad (4)$$

where V_{m0} is the MPI, V_m is the quasi-steady-state maximum tangential wind of a model simulation. The relation shown in equation (4) suggests that a TC with a larger M_m has more SI given the same environment (the same a_0 , a , and b). This SI index is also a good indicator for the magnitude of supergradient winds. Given the same environment, the SI trend from equation (4) is consistent with the degree of gradient wind imbalance (GIB) estimated in Miyamoto et al. (2014) that a TC with a larger r_m will have larger GIB. At the same time, with less turbulent mixing (smaller a and b), the value of SI is larger and the wind field will become more supergradient as shown in Bryan (2012). From another perspective, equation (4) allows the comparison of the SI for different model setups and environmental factors through the comparison of the corresponding a_0 , a , and b .

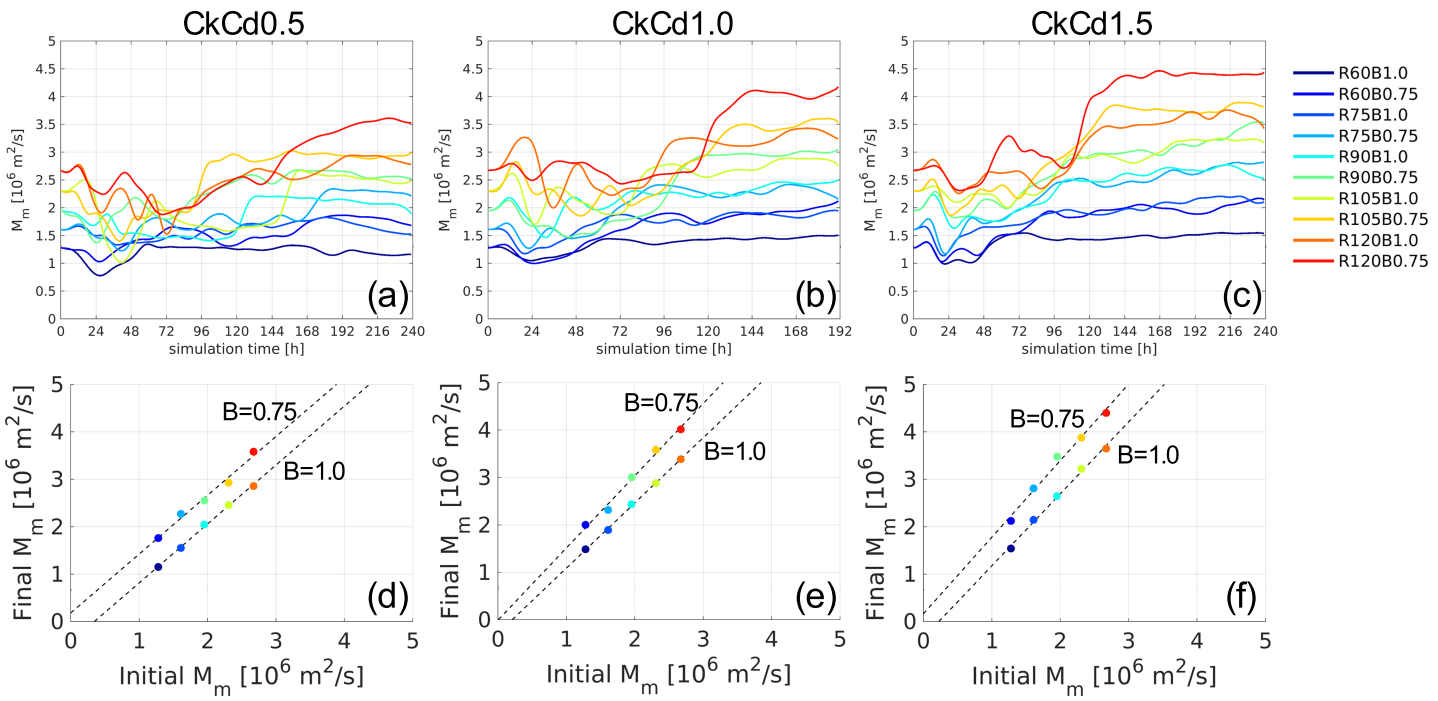


Figure 5. (a–c) Time evolutions of M_m at $z = 1.55 \text{ km}$. (d–f) Dots are the final 24-hr mean of M_m as a function of initial M_m . Dash lines are the linear regression of the dots with the same B value. (left column) CkCd0.5. (middle column) CkCd1.0. (right column) CkCd1.5.

4. Summary and Discussion

This study seeks to know the relations among M_m , r_m and V_m in the model simulations of TCs under the same environmental conditions, and what causes the discrepancy between the MPI theories and model simulations. Although the relationship between the TC size and intensity has been explored by some studies (Merrill, 1984; Xu & Wang, 2010), the complex external and internal factors conceal the relationship between them. In the present paper, we find through the analysis of suite of idealized numerical simulations that at the steady state the radius of maximum wind (r_m) above the boundary layer top has a linear relationship ($r_m = aM_m + b$) with the absolute angular momentum M_m that passes through r_m . The nonnegligible r_m intercept b provides a way to understand why storms with larger M_m and larger r_m are more intense at the steady state in model simulations. The balanced axisymmetric theories for steady-state tropical cyclone predict a linear relationship where a would be based on differing environmental conditions, but a nonzero r_m intercept b is not expected from those theories. It is found here that the horizontal turbulent mixing is responsible for the existence of this nonzero b , and that a can depend on turbulent mixing as well as environmental conditions and $\frac{C_k}{C_d}$. The role of horizontal turbulent mixing on modulating the final maximum intensities is through adjusting the linear relationship between r_m and M_m and that less horizontal turbulent mixing will produce both smaller slope a (greater V_m) and intercept b . Though only the sensitivities of $\frac{C_k}{C_d}$ and horizontal turbulent mixing length are tested here, additional tests with varying sea surface temperature and microphysics (not shown) confirm similar linear relationships and we expect the results to hold under different specified environmental and model setups. This linear relationship shows that the processes not included in the balanced axisymmetric TC theories do not completely contaminate the theoretical results but rather modify the relationship. Furthermore, this finding also provides a way to quantify the ratio of the supergradient wind attributed to the processes not included in the classic MPI theory.

The results shown in section 3 can have important practical applications in modeling and forecasting. We have found in the present study the characteristics of the simulated maximum intensity and the radius of maximum wind for quasi-steady-state tropical cyclones under a given environment. Thus, if we can relate the final state to the storm's initial state, we will be able to predict some of the important storm parameters

to some extent. Figure 5 shows that although M_m is not conserved during development (first row of Figure 5), a larger initial M_m tends to have a larger final M_m (second row of Figure 5). This positive correlation between the initial M_m and final M_m tells us that the final storm structure and intensity have some memory of the initial vortex structure and intensity. Another interesting finding from Figure 5 is that the storms with the smaller initial M_m tends to keep its M_m closer to its original value compared to the larger initial M_m storms. We believe this to be partially related to the fact that storms with larger initial M_m need a longer time to reach a quasi-steady-state (first row of Figure 2), which then increases the possibility of environmental influence during its development stage.

It is also shown in the second row of Figure 5 that the parameter B (controlling the skirt outside r_m) has an effect on the final M_m : given the same initial r_m , the storms with a smaller B value (broader vortex), will have a larger final M_m compared to the storms with a larger B value. However, the B parameter can be changed by the environmental influence during the storm's early development stage, that is, the modification of sea surface temperature (Sun et al., 2017) and environmental moisture (Hill & Lackmann, 2009) on the moist convections in the rainbands and hence the storm wind structure outside r_m . Further exploration of the relationships between initial and final vortex structure in a variety of environmental conditions is warranted and will be the subject of future research.

Acknowledgments

Authors D. Tao and M. Bell are supported by grant Office of Naval Research award N000141613033 and National Science Foundation (NSF) award AGS-1701225. The contribution of R. Rotunno to this work is supported by the National Center for Atmospheric Research, which is a major facility sponsored by the National Science Foundation under cooperative agreement 1852977. P.J. van Leeuwen is supported by Colorado State University. Computing was performed at a local computer server at the Department of Atmospheric Science, Colorado State University. The data used in this paper are available through zenodo using the link <https://doi.org/10.5281/zenodo.3530892>.

References

- Bryan, G. H. (2012). Effects of surface exchange coefficients and turbulence length scales on the intensity and structure of numerically simulated hurricanes. *Monthly Weather Review*, 140, 1125–1143. <https://doi.org/10.1175/MWR-D-11-00231.1>
- Bryan, G. H. (2013). Comments on sensitivity of tropical-cyclone models to the surface drag coefficient. *Quarterly Journal of the Royal Meteorological Society*, 139, 1957–1960. <https://doi.org/10.1002/qj.2066>
- Bryan, G. H., & Rotunno, R. (2009). The maximum intensity of tropical cyclones in axisymmetric numerical model simulations. *Monthly Weather Review*, 137, 1770–1789. <https://doi.org/10.1175/2008MWR2709.1>
- Carrasco, C. A., Landsea, C. W., & Lin, Y. (2014). The influence of tropical cyclone size on its intensification. *Weather and Forecasting*, 29, 582–590. <https://doi.org/10.1175/WAF-D-13-00092.1>
- Chan, K. T. F., & Chan, J. C. L. (2014). Impacts of initial vortex size and planetary vorticity on tropical cyclone size. *Quarterly Journal of the Royal Meteorological Society*, 140, 2235–2248. <https://doi.org/10.1002/qj.2292>
- Emanuel, K., & Rotunno, R. (2011). Self-stratification of tropical cyclone outflow. Part I: Implications for storm structure. *Journal of the Atmospheric Sciences*, 68, 2236–2249. <https://doi.org/10.1175/JAS-D-10-05024.1>
- Emanuel, K. A. (1986). An air-sea interaction theory for tropical cyclones. Part I: Steady-state maintenance. *Journal of the Atmospheric Sciences*, 43, 585–605. [https://doi.org/10.1175/1520-0469\(1986\)043<0585:AASITF>2.0.CO;2](https://doi.org/10.1175/1520-0469(1986)043<0585:AASITF>2.0.CO;2)
- Emanuel, K. A. (1988). The maximum intensity of hurricanes. *Journal of the Atmospheric Sciences*, 45, 1143–1155. [https://doi.org/10.1175/1520-0469\(1988\)045<1143:TMIOH>2.0.CO;2](https://doi.org/10.1175/1520-0469(1988)045<1143:TMIOH>2.0.CO;2)
- Emanuel, K. A. (1995). Sensitivity of tropical cyclones to surface exchange coefficients and a revised steady-state model incorporating eye dynamics. *Journal of the Atmospheric Sciences*, 52, 3969–3976. [https://doi.org/10.1175/1520-0469\(1995\)052<3969:SOTCTS>2.0.CO;2](https://doi.org/10.1175/1520-0469(1995)052<3969:SOTCTS>2.0.CO;2)
- Emanuel, K. A. (1997). Some aspects of hurricane inner-core dynamics and energetics. *Journal of the Atmospheric Sciences*, 54, 1014–1026. [https://doi.org/10.1175/1520-0469\(1997\)054<1014:SAOHIC>2.0.CO;2](https://doi.org/10.1175/1520-0469(1997)054<1014:SAOHIC>2.0.CO;2)
- Hill, K. A., & Lackmann, G. M. (2009). Influence of environmental humidity on tropical cyclone size. *Monthly Weather Review*, 137, 3294–3315. <https://doi.org/10.1175/2009MWR2679.1>
- Merrill, R. T. (1984). A comparison of large and small tropical cyclones. *Monthly Weather Review*, 112, 1408–1418. [https://doi.org/10.1175/1520-0493\(1984\)112<1408:ACOLAS>2.0.CO;2](https://doi.org/10.1175/1520-0493(1984)112<1408:ACOLAS>2.0.CO;2)
- Miyamoto, Y., Satoh, M., Tomita, H., Oouchi, K., Yamada, Y., Kodama, C., & Kinter, J. (2014). Gradient wind balance in tropical cyclones in high-resolution global experiments. *Monthly Weather Review*, 142, 1908–1926. <https://doi.org/10.1175/MWR-D-13-00115.1>
- Peng, K., Rotunno, R., & Bryan, G. H. (2018). Evaluation of a time-dependent model for the intensification of tropical cyclones. *Journal of the Atmospheric Sciences*, 75, 2125–2138. <https://doi.org/10.1175/JAS-D-17-0382.1>
- Rotunno, R., & Bryan, G. H. (2012). Effects of parameterized diffusion on simulated hurricanes. *Journal of the Atmospheric Sciences*, 69, 2284–2299. <https://doi.org/10.1175/JAS-D-11-0204.1>
- Rousseau-Rizzi, R., & Emanuel, K. (2019). An evaluation of hurricane superintensity in axisymmetric numerical models. *Journal of the Atmospheric Sciences*, 76, 1697–1708. <https://doi.org/10.1175/JAS-D-18-0238.1>
- Shutts, G. J. (1981). Hurricane Structure and the Zero Potential Vorticity Approximation. *Monthly Weather Review*, 109, 324–329. [https://doi.org/10.1175/1520-0493\(1981\)109<0324:HSATZP>2.0.CO;2](https://doi.org/10.1175/1520-0493(1981)109<0324:HSATZP>2.0.CO;2)
- Sun, Y., Zhong, Z., Li, T., Yi, L., Hu, Y., Wan, H., et al. (2017). Impact of ocean warming on tropical cyclone size and its destructiveness. *Scientific Reports*, 7(1), 8154. <https://doi.org/10.1038/s41598-017-08533-6>
- Xu, J., & Wang, Y. (2010). Sensitivity of the simulated tropical cyclone inner-core size to the initial vortex size. *Monthly Weather Review*, 138, 4135–4157. <https://doi.org/10.1175/2010MWR3335.1>
- Xu, J., & Wang, Y. (2015). A statistical analysis on the dependence of tropical cyclone intensification rate on the storm intensity and size in the North Atlantic. *Weather and Forecasting*, 30, 692–701. <https://doi.org/10.1175/WAF-D-14-00141.1>
- Xu, J., & Wang, Y. (2018). Effect of the initial vortex structure on intensification of a numerically simulated tropical cyclone. *Journal of the Meteorological Society of Japan*, 96, 111–126. <https://doi.org/10.2151/jmsj.2018-014>
- Zhang, J. A., & Marks, F. D. (2015). Effects of horizontal diffusion on tropical cyclone intensity change and structure in idealized three-dimensional numerical simulations. *Monthly Weather Review*, 143, 3981–3995. <https://doi.org/10.1175/MWR-D-14-00341.1>